Spin-Resolved Electronic Structure of Nanoscale Cobalt Islands on Cu(111)

O. Pietzsch,[1,*] S. Okatov,[2] A. Kubetzka,[1] M. Bode,[1] S. Heinze,[1] A. Lichtenstein,[2] and R. Wiesendanger[1]

[1]*Institute of Applied Physics, University of Hamburg, Jungiusstrasse 11, D-20355 Hamburg, Germany*

[2]*I. Institute of Theoretical Physics, University of Hamburg, Jungiusstrasse 9, D-20355 Hamburg, Germany*

(Received 2 March 2006; published 15 June 2006)

Using spin-polarized scanning tunneling spectroscopy, we reveal how the standing wave patterns of confined surface state electrons on top of nanometer-scale ferromagnetic Co islands on Cu(111) are affected by the spin character of the responsible state, thus experimentally confirming a very recent theoretical result [L. Niebergall *et al.*, Phys. Rev. Lett. **96**, 127204 (2006)]. Furthermore, at the rim of the islands a spin-polarized state is found giving rise to enhanced zero bias conductance. Its polarization is opposite to that of the islands. The experimental findings are in accordance with *ab initio* spin-density calculations.

DOI: 10.1103/PhysRevLett.96.237203 PACS numbers: 75.75.+a, 68.37.Ef, 71.15.Mb, 73.20.At

Standing wave patterns arising from scattering of surface state electrons off defects like terrace edges, impurities or adsorbates have aroused continued high attention in surface science since their first observation on densely packed noble metal surfaces more than ten years ago [1,2]. These quantum interference phenomena can be observed by scanning tunneling microscopy (STM) as a lateral periodic modulation of the local density of states (LDOS). Magnetic materials have been used as adsorbates [3,4] or adlayers [5,6] in a number of studies. The STM data published so far, however, were not spin resolved. The only exception, to our knowledge, is a recent study reporting on a variation of standing wave patterns on oppositely magnetized domains of ultrathin Fe films [7].

Nanometer-scale Co islands on the Cu(111) surface establish a particularly interesting system, because both substrate and islands exhibit their own standing wave patterns, expected to be spin polarized in one material but not in the other. This system has been investigated in some detail by scanning tunneling spectroscopy (STS) and *ab initio* calculations [6]. Extracting the parallel wave number $k_{\|}$ from differential conductance maps the dispersion relation of the Co surface state was derived. Theoretical calculations identified two main surface related electronic features, namely, a very strong and narrow LDOS peak caused by an occupied d_{z^2}-like state of minority spin character, and a mostly unoccupied s-p-like dispersive band of majority spin character, the latter being responsible for the LDOS standing wave patterns. However, the experimental data were not spin resolved.

In subsequent work utilizing spin-polarized scanning tunneling spectroscopy (SP-STS) the Co islands were identified as ferromagnetic, exhibiting a perpendicular magnetization with strong coercivity and remanence [8]. Also, recent theoretical work [9] confirmed the minority spin character of the peak and gave evidence that its existence is a property of the Co surface, independent of the Cu substrate. The Co standing wave patterns were revisited in a very recent theoretical study [10], published after first submission of this Letter, predicting the standing waves to occur exclusively in the spin-up but not in the spin-down LDOS.

In this Letter we present low temperature SP-STS investigations of the Co surface electronic structure. Focus is put particularly on the energy range in which the standing wave patterns can be observed on the Co islands, that is, at energies above that of the sharp minority peak, extending well into the unoccupied states. Furthermore, in narrow rim regions bounding the Co islands a spin-polarized state is observed which gives rise to an enhanced zero bias conductance. The spin character of this rim state is opposite to that exhibited by the island at the corresponding energy, emphasizing that the spin polarization, on a lateral scale of a few angstroms, *may not only change its magnitude but also its sign*, depending on the electronic states involved.

The experiments were performend in a multichamber system allowing all preparation steps of sample and tip to be carried out in UHV conditions [11]. The Cu(111) single crystal was cleaned by repeated cycles of Ar^+ sputtering and anneal to 600 °C. Nominally, 0.6 monolayers of Co were evaporated at room temperature with no further anneal, resulting in triangular Co islands protruding 2 atomic layers high from the Cu surface. The sample was inserted into the cryogenic microscope immediately after termination of the Co deposition (typical transfer time 2.5–3 min) and rapidly cooled down to the measurement temperature of 14 K to suppress intermixing or Cu capping. We used a polycrystalline W tip coated with an antiferromagnetic Cr film of 75 ± 50 ML thickness which was checked for sensitivity to the perpendicular sample magnetization component on the well-known system of Fe/W(110) double-layer stripes [12]. The tip was stabilized at a sample voltage of $U_{\mathrm{stab}} = +0.6$ V and a tunneling current of $I_{\mathrm{stab}} = 1$ nA. With the feedback loop open, the bias voltage U was ramped between $+0.5$ V and -1 V and the differential conductance $dI/dU(U)$ was measured by a lock-in technique. This signal is approximately proportional to the LDOS at the position of the tip [13]. In this way tunneling spectra were taken at each pixel of the image. All images shown in this Letter are maps taken from the three-

dimensional $dI/dU(x, y, eU)$ stack of data, where $eU = E - E_F$ determines the energy relative to the Fermi level.

In Figs. 1(a) and 1(b) we show $dI/dU(U)$ maps at bias voltages allowing to observe the standing wave patterns on both the Cu substrate and on the Co islands. The contrasts between islands are due to their magnetization being oriented either up or down, that is, parallel or antiparallel to the tip magnetization, respectively. The contrast inversion between (a) and (b) is *not* caused by a magnetization reversal of either tip or sample, but is the result of contributions to the LDOS from states of opposite spin, their relative weights depending on the applied bias voltage. The chromium at the tip has an electronic structure dominated by minority spin states near the Fermi level [14], allowing a very effective tunneling between tip and sample minority states if tip and island are in a parallel magnetic configuration. The bias voltage of Fig. 1(a) has been chosen, however, in a range where the main contribution to the sample LDOS comes from the dispersive *majority* spin state which is responsible for the standing wave pattern. Therefore, the islands exhibit an *inverted* contrast. In Ref. [6] the onset of this band was determined to -0.16 eV from a fit of the dispersion relation. Our own data suggest an even lower band edge energy. A first faint oscillation pattern can already be discerned at -0.184 eV [15], and from a parabolic fit, see the inset of panel (c), we arrive at an onset as low as -0.22 eV. Initially, this state has not enough weight to be detected by tunneling spectroscopy in the tail of the huge minority spin peak close to -0.3 eV, and a contrast inversion of the Co islands indicating a sign reversal of SP is delayed to -0.065 eV, i.e., still below the Fermi level. Towards higher energies, the majority spin band is the predominant electronic feature of the Co island surface and keeps this role in a wide energy range extending well into the unoccupied states. There is, however, a narrow energy region in which the islands return to *normal* spin contrast as exemplified in Fig. 1(b). In our data, this is between 0.18 eV and 0.43 eV above E_F. In this interval again an unoccupied localized minority spin *d* state outweighs the majority band. Interestingly, Barral *et al.*, without discussing this detail, find a flat *d* band and a corresponding peak in their calculated minority spin vacuum DOS in this energy region [9]. Figure 1(c) also shows the effect of electron confinement, manifest in the evolution of the standing wave periods as a function of bias voltage. The steplike structure of the data reflects the occurrence of discrete resonant states, see also Ref. [15]. The inset of Fig. 1(c) allows for a comparison of the dispersive behavior of Co and the Cu surface. Both data sets were fit (solid lines) assuming a 2D free electron gas, confined for Co but not for Cu: while the Cu values smoothly match the fit parabola, the Co data again display a steplike structure.

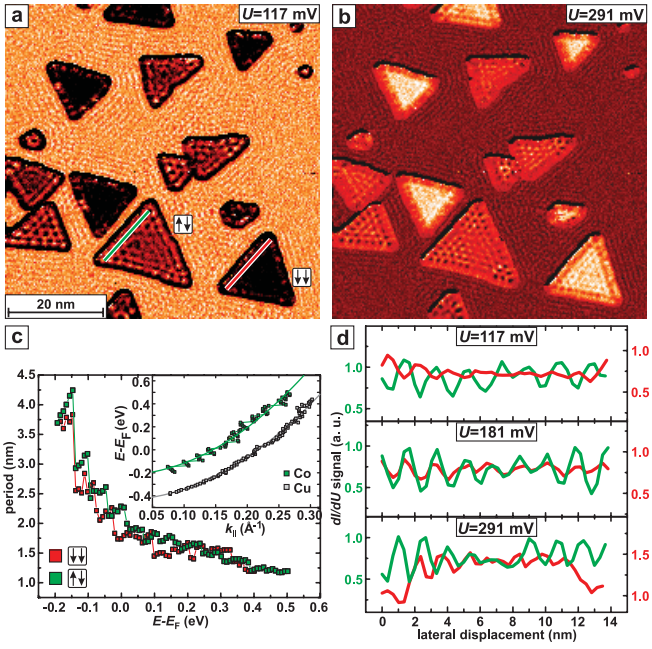

FIG. 1 (color). 0.6 ML Co on Cu(111). (a), (b) dI/dU maps at sample bias voltages as indicated, showing standing wave patterns on both Cu substrate and Co islands. Arrows indicate islands being magnetized parallel (⇊) or antiparallel (⇅) to the tip magnetization. (c) Standing wave periods on Co islands as a function of bias voltage. Inset: E vs $k_{\|}$ for Co islands and Cu surface. Solid lines: parabolic fits. (d) dI/dU profiles taken along lines as indicated in (a), at corresponding color coding. Regardless of the bias voltage, the standing wave amplitude is larger on the antiparallel island.

The effect of SP on the Co patterns is displayed in Fig. 1(d). We show dI/dU profiles, taken along lines as indicated in Fig. 1(a) for bias voltages being representative for ranges of inverse, balanced, and normal spin contrast. In each case the standing wave amplitude is found significantly larger on the antiparallel island, regardless of the sign of the bias dependent SP. The amplitude ratios of the parallel and antiparallel case are 0.49, 0.40, and 0.32 at the respective voltages. Qualitatively, this behavior is explained as follows: Because the tip has an effective *negative* SP within the energy range relevant for the standing wave observation, tunneling into the oscillatory *majority* surface state band is not very efficient for the parallel configuration. On the other hand, in antiparallel magnetized islands, the role of minority and majority spins, as referenced from the tip's perspective, is exchanged. As a consequence, the oscillatory state in antiparallel islands has the matching spin character for an effective tunneling of the excess tip minority spin electrons, resulting in an enhanced scattering amplitude. Only delocalized sample majority electrons take part in the LDOS oscillations while localized minority *d*-like electrons do not. Still, the net balance of contributions from majority and minority states to the sample LDOS determines the overall contrast between the islands which may be normal or inverted (or balanced at the point of sign inversion), depending on the bias voltage; the standing wave pattern is then superimposed onto this background signal.

Within our lateral and energy resolution, we do not observe any spin-induced modification of the Cu oscillation pattern in the immediate vicinity of oppositely magnetized Co islands. However, there is a remarkable feature found in the islands' rims. All islands are bounded by a rim area with a typical apparent width of 1.7 ± 0.2 nm, i.e., several atomic rows wide, as determined from both topographic and dI/dU images. In constant current images (not shown) this rim exhibits an increased apparent height, amounting to an enhancement of up to 55 pm at small bias voltages. These rim areas have an electronic structure being clearly different from that of the islands' interior. In particular, right at the Fermi energy we observe a striking enhancement of the local differential conductance at the rim, see the insets of Fig. 2 at a bias voltage $U = -1$ mV. We have taken spectra inside the white box shown in the right inset, with the box spanning parts of the island, the rim itself, and the Cu surface. Each spectral curve of the series numbered 1–11 in Fig. 2 (shifted vertically for clarity) samples 4–6 pixels along a line parallel to the short box edge, with consecutive equidistant lines progressing from the Co island (curve 1) through the rim area to the Cu substrate (curve 11). We have labeled by capital letters (A–D) some features particularly characteristic for the different materials. Here (A) is the steep onset of the Cu surface state, and (B) is the large d-like peak of the Co islands. Progressing from the Co island surface into the rim region, feature (B) is strongly attenuated and eventually fades out (curves 1 through 6). The rim area is represented by curves 4–8. Starting at curve 4 a new peak (C) emerges which becomes maximal in curves 6 and 7 and vanishes beyond curve 8. This peak is energetically located right at the Fermi energy and is found neither in the inner Co island nor in Cu. It is the hallmark of the rim. Curves 9–11 clearly identify the Cu substrate surface. Peak (D) is caused by the unoccupied minority state mentioned above. It is observed on Co as well as in the rim area but is completely absent on Cu. From this latter observation we conclude that the rim area mainly consists of Co and not of Cu.

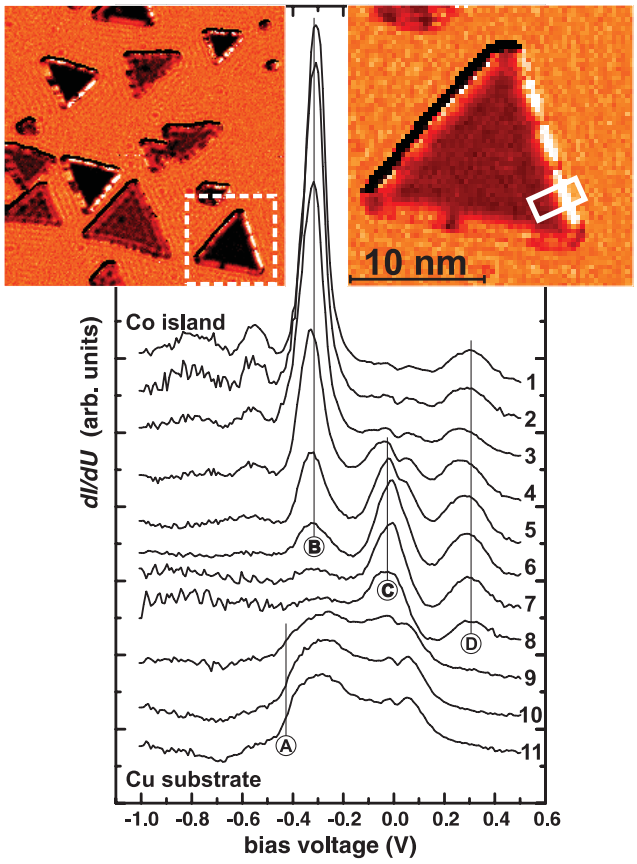

FIG. 2 (color). Enhanced zero bias conductance in the rim area of the parallel island. Spectral curves (vertically shifted for clarity) were measured inside the white box in the right inset. Labels (A), (B), (C), (D) mark characteristic features: (A) onset of the Cu surface state, (B) sharp d-like peak of the Co islands which is strongly attenuated in the rim area, (C) zero bias peak existing exclusively in the rim area, (D) minority spin peak observed on the Co island as well as in the rim area but not on Cu.

As is already obvious from inspecting the left inset of Fig. 2, not all islands show an equally bright rim at zero bias. In Fig. 3(a) we compare the rim spectrum of the parallel island to a corresponding location of the antiparallel island. The latter exhibits again a peak at the Fermi level but with significantly lower intensity. Thus, the rim state is clearly found to be spin-polarized. Remarkably, the spin contrast at this energy is *normal* for the rim while it is *inverse* for the islands; see the asymmetry plots in Fig. 3(b). At zero bias, the islands exhibit an asymmetry of -13% while it amounts to $+24\%$ in the rim. The left inset of Fig. 2 clearly shows that all dark islands (i.e., the

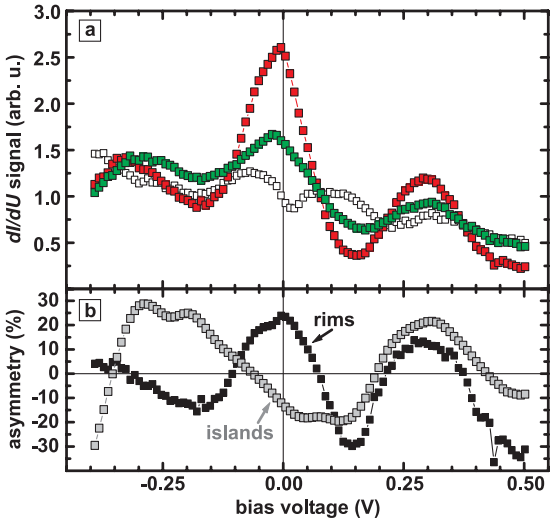

FIG. 3 (color). (a) Rim state at parallel (red) and antiparallel (green) islands. The peaks are those labeled (C) and (D) in Fig. 2. Hollow squares: strongly reduced conductance at zero bias at dark spots inside the rim. (b) dI/dU asymmetries at rims (black) and at inner parts of islands (gray). At zero bias the respective signs are opposite.

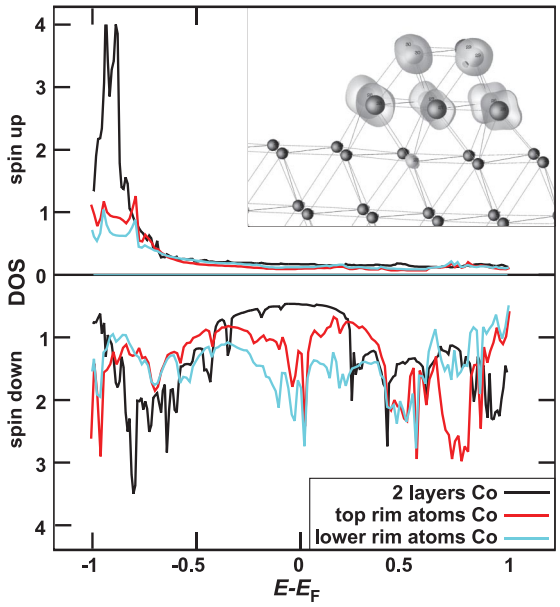

FIG. 4 (color). Comparison of calculated DOS of an extended 2 layers Co film (black) and of rim sites (blue, lower atom; red, upper atom). The rim exhibits a d-like minority peak structure at the Fermi level which is absent off the rim. Inset: Charge density from integration over the energy interval -0.1 eV $< E - E_F <$ 0.1 eV. Only rim atoms contribute to the peak at E_F.

parallel ones) display the enhanced zero bias conductance in their rims. This observation indicates that the islands' electronic structure in this energy window is dominated by majority spin contributions whereas that of the rim has minority spin character. In this context it is noteworthy that the images also reveal some degree of inhomogeneity in the rim areas showing up as dark spots interrupting the bright lines; see, e.g., the insets of Fig. 2. In the corresponding spectra we observe a strong intensity reduction or even a dip at the energetic position of the zero bias peak cf. the hollow squares in Fig. 3(a). A tentative explanation would be a locally varying degree of intermixing of Co and Cu atoms [16].

We have performed *ab initio* electronic structure calculations of the Co island rim in comparison to an ideal 2 ML Co film, using the projected augmented wave method [17,18] in the framework of density functional theory, applying the generalized gradient approximation [19]. The Brillouin zone is sampled as a $2 \times 16 \times 1$ mesh with its origin at the Γ point. The valence states include $3d$, $4s$ for both Cu and Co atoms. The cutoff energy of the plane-wave expansion is 342 eV. The Co island rim on the Cu(111) surface is calculated in the model of a 7-layer slab, containing 5 layers of the Cu substrate of 5 atoms in size and 2 layers of Co with 3 (lower layer) and 2 (topmost) atoms. A full ionic relaxation has been made. In Fig. 4 we present the DOS calculated for the muffin tins.

The central result is a peak structure found right at the Fermi energy for the rim atoms which is completely absent on the extended Co surface. The responsible state is of d character and has minority spin. Orbitals with d_{z^2}, d_{xz}, d_{yz} symmetry provide almost equal weight; lower rim atoms exhibit a DOS roughly twice that of the top atoms. The inset of Fig. 4 displays the charge density distribution, as obtained from integration over an energy interval -0.1 eV $< E - E_F < 0.1$ eV. Contribution to the zero bias peak is found exclusively at the rim atoms. The calculated results nicely agree with the experimental observations.

In conclusion, at a lateral scale of only a few angstroms the SP may not only change in magnitude but also may reverse its sign. In magnetic structures only a few nanometers in size such local effects increasingly gain weight and may eventually lead to unexpected size dependent effects.

Financial support from the DFG (Grants No. Wi 1277/19-1 and No. SFB 668-A8) is gratefully acknowledged. S. H. additionally thanks the Stifterverband für die Deutsche Wissenschaft and the Interdisciplinary Nanoscience Center Hamburg for financial support.

*Email address: pietzsch@physnet.uni-hamburg.de; Electronic address: http://www.nanoscience.de/group_r/stm-spstm/

[1] Y. Hasegawa and P. Avouris, Phys. Rev. Lett. **71**, 1071 (1993).
[2] M. F. Crommie, C. P. Lutz, and D. M. Eigler, Nature (London) **363**, 524 (1993).
[3] M. F. Crommie, C. P. Lutz, and D. M. Eigler, Science **262**, 218 (1993).
[4] H. C. Manoharan, C. P. Lutz, and D. M. Eigler, Nature (London) **403**, 512 (2000).
[5] S. Pons, P. Mallet, and J.-Y. Veuillen, Phys. Rev. B **64**, 193408 (2001).
[6] L. Diekhöner *et al.*, Phys. Rev. Lett. **90**, 236801 (2003).
[7] K. von Bergmann *et al.*, Phys. Rev. Lett. **92**, 046801 (2004).
[8] O. Pietzsch *et al.*, Phys. Rev. Lett. **92**, 057202 (2004).
[9] M. A. Barral, M. Weissmann, and A. M. Llois, Phys. Rev. B **72**, 125433 (2005).
[10] L. Niebergall *et al.*, Phys. Rev. Lett. **96**, 127204 (2006)
[11] O. Pietzsch *et al.*, Rev. Sci. Instrum. **71**, 424 (2000).
[12] A. Kubetzka *et al.*, Phys. Rev. Lett. **88**, 057201 (2002).
[13] J. Tersoff and D. R. Hamann, Phys. Rev. B **31**, 805 (1985).
[14] C. Rau and S. Eichner, Phys. Rev. Lett. **47**, 939 (1981).
[15] See EPAPS Document No. E-PRLTAO-96-064625 for an animated sequence of the evolution of contrasts and standing wave patterns as functions of bias voltage. For more information on EPAPS, see http://www.aip.org/pubservs/epaps.html.
[16] The variation in brightness of differently oriented island edges is most likely caused by an asymmetric tip geometry.
[17] G. Kresse and D. Joubert, Phys. Rev. B **59**, 1758 (1999).
[18] P. E. Blöchl, Phys. Rev. B **50**, 17 953 (1994).
[19] J. P. Perdew and Y. Wang, Phys. Rev. B **45**, 13 244 (1992).